World Conference on Timber Engineering Oslo 2023

DYNAMIC PERFORMANCE OF A FULL-SCALE WOOD FRAME SUBJECTED TO CYCLIC LOAD TESTING

Félix Bouffard[1], Jean Proulx[2]

ABSTRACT: The strength-to-weight ratio of wood structural elements makes them very attractive on an engineering design point of view. This is one of the reasons why wooden buildings are known to perform well during seismic events of medium and high intensities. However, ductility and over strength factors, making it possible to design structures having the capacity to resist a seismic event by its inelastic properties, are not well characterized and leads to a local over design of assemblies and critical wood sections. The primary objective of this study is to characterize the cyclic behaviour of a diagonally braced full-scale frame. This study focuses on capacity design to have the dowel assemblies as the main dissipator of energy. A full-size frame specimen was subjected to cyclic loading. The frame was built with glulam timber elements joined together with hidden steel plates and fastened with dowels. The cyclic loading results demonstrated a global ductile behaviour, a good redistribution of the internal efforts in the assemblies, a reduction of the secant stiffness after the yielding point, increment of the dissipation of energy, great over-strength, and minor damage in the timber elements. This supports the use of this type of frame with a capacity design focused on a ductile behaviour.

KEYWORDS: Seismic behaviour, Full-scale, Wood frame, Cyclic loading, Glulam, Capacity design, Seismic force resisting system

1 BACKGROUND AND MOTIVATION

Various research studies have been conducted on wood as a material, and there is a greater understanding of its mechanical properties. It is now possible to use wood and to manufacture it in such a way as to obtain structural products with a mechanical resistance increasingly comparable to that of steel, and allowing to build high rise buildings. On a structural engineering point of view, wood is a very light and strong material. Therefore, wooden buildings perform relatively well during seismic events of medium and high intensities. However, wood as a material possesses low ductility properties and brittle failure modes. The National Building Code of Canada (NBCC) [1] is giving more room to allow the design and construction of all-wood Seismic Force Resisting Systems (SFRS) into new buildings. When designing engineered wood structures, ductility and over-strength factors are used. These coefficients, making it possible to design structures entirely in wood having the capacity to resist a seismic event by its inelastic properties, are very low. The problem is that a low global demand stemming from small, underdeveloped force modification factors leads to a local over design of connections and critical wood sections. SFRS built entirely from engineered wood therefore require more material for compliance purposes. In the NBCC, the R_d factor considers the ductility of the system and its ability to absorb energy, and the R_o factor considers the overstrength of the structure.

Due to the increasing use of timber braced frame in practice, multiple configurations of these systems were developed, and this leads to new questions. Previous research [2]–[5] has been conducted to evaluate the behaviour of such systems, investigating the influence of capacity design, connection behaviour, brace configuration as well as the protocols used for cyclic testing. The behaviour of timber braced frames is generally highly influenced by its energy absorption capacity and overall ductility which is governed by a proper design [2]. The main components of interest in capacity design of such structures are generally the connections in the joints, as there is existing knowledge on ductile failure modes. Connectors type and their configuration in wood elements directly influence the behaviour of local wood to steel assemblies and the overall behaviour of a structure [3]. Braced frames with diagonal wood elements have been tested in different configurations to evaluate their performance. Frames with X-brace or K-brace were shown to have desirable lateral stiffness and can be improved with a design focused on ductile failure modes [5]. On a global perspective, other researchers focused their attention on cyclic protocols used to ensure proper characterization of timber frames. Cyclic testing patterns with sequences composed of multiple cycles can be demanding in terms of the effects on the results. It is therefore important to have a representative loading protocol that simulates the behaviour of a real seismic energy demand to correctly establish the properties of interest [4].

The literature review emphasized the need for studies on the dynamic performance of a full-scale braced frame designed according to industry standards, which would give information to professionals in regards of the critical parameters to be used for design. The primary objective of this study is to characterize the cyclic behaviour of a diagonally braced frame of a three-storey wooden building and identify the current design challenges. The full-size specimen is a braced frame with a diagonal glulam wood element connected with two dowel

[1] Félix Bouffard, University of Sherbrooke, Canada, felix.bouffard@usherbrooke.ca

[2] Jean Proulx, University of Sherbrooke, Canada, jean.proulx@usherbrooke.ca

https://doi.org/10.52202/069179-0269

assemblies that are designated to be the fuses in accordance with the principle of capacity design.
A testing methodology was established with suitable properties for a full-scale loading protocol in the structural laboratory of the University of Sherbrooke. This test allowed for the analysis of the energy dissipation capacity, resistance parameters and lateral stiffness of the frame. The results of this research provides information on how to approach such problems and behavioural data for future research.

2 APPROACH

2.1 STANDARD WOOD BUILDING

To incorporate elements that would be observed in an actual timber construction, the fictional "benchmark" building proposed by the Canadian Wood Council (CWC) [6], as shown in Figure 1, was used as a reference. This three-storey building is 12.192 m high, has a ground area of approximately 1440 m^2 and a typical grid spacing of 7.62 m by 7.62 m in each direction. Using SAP2000 [7] and S-Frame [8], the building was modelled and analysed to find the critical load combination, including seismic and snow loads.. The use of different commercial software allowed for a verification of the results to ensure reliable loading targets for laboratory testing. The numerical analysis showed that the critical SFRS was on the long side of the building. The equivalent static load method for a building located in Montréal (City Hall), Canada on a class C soil was used to establish the applied seismic force. The uniformly distributed roof loads are 1.5 kPa and 2.3 kPa for dead load and snow load respectively. For the floors, the uniformly distributed loads are 3 kPa and 2.4 kPa for dead load and live load, respectively. In the context of this research, the R_d and R_o factors for such a structure were chosen to be 2.0 and 1.5 for a moderately ductile system with ductile connections respectively. The total hypothetical weight of the building was assumed to be 11204 kN resulting in a lateral seismic force at ground level of 1481 kN. Accidental torsion was considered during the redistribution of the seismic force in each storey. These forces were then reproduced on the specimen with the experimental setup.

Figure 1: *Standard wood building by the CWC*

2.2 FRAME DESIGN

Due to the fragile properties of wood, there must be pre-assigned ductile elements that will yield firstly to impose a safety measure. All elements that must be oversized compared to an unprotected element are non-energy dissipating elements. The specimen of this research was designed using the capacity design approach. This allowed to pre-determine the components that would fail first. Therefore, all the elements, except for the two dowel assemblies in the brace element were overdesigned to have a linear deformation behaviour. To determine the appropriate geometry of the non-dissipating elements of the specimen, a reduction of the seismic force based only on the overstrength factor was used. As for the ductile assembly, its design was based on the CSA O86-14 adapted the European model [9] for ductile deformation of steel connectors in wood. Both reduction factors accounting for overstrength, and ductility were used to reduce the seismic force for the dowel connections design. The "g" mode was prioritized to be the governing mode of deformation to fully utilize the yield of the dowels and the crushing of the wood.

2.3 CONNECTION STIFFNESS ASSUMPTIONS

During the design phase of the specimen, the challenge was the determination of the connection properties. Since bracing systems, similar to the one in this research, are usually composed of two steel to wood connections and a diagonal element, they have a direct influence on the total drift of the SFRS. The problem is that the stiffness of these connections is not documented by Canadian standards, which means that professionals must rely on values that are not necessarily representative of values that could be observed in the field. This leads to a misrepresentation of the drift ratio of wood SRFS in large-scale buildings.
To solve this issue, the slippage modulus, K_{ser}, established in the SIA 265 standard [10] and by the Eurocode 5 (E5) [11] was used to characterize the stiffness and the drift of the specimen. For Canadian SPF 12c-E class wood, the density of $\rho = 455\ kg/m^3$ was used according to the CSA O86-14 standard. Drift displacement of the whole system was assumed by using the relationship of derivation of connection and system stiffness developed by Chen and Popovski [12].

3 FULL-SCALE WOOD FRAME

3.1 MATERIALS

All the timber elements were joined with grade 350W steel plates and fastened with grade A325 dowels in respect of the ASTM standards. The steel plates connecting the braced assembly were 19.1 mm thick and the column plate were 12.7 mm thick. The 56 dowels (28 at each end) connecting the brace element had a diameter of 9.5 mm and the other 53 dowels had a diameter of 19.1 mm. All the dowels had a length of 342.9 mm. They were hammered in place, as per typical on-site instructions. Yield point of all steel elements was 310 MPa. All the requirements from CSA S16-14 [13] were considered during the design phase of these elements. All the wood members were made of glued laminated Canadian spruce-

https://doi.org/10.52202/069179-0269

pine-fir (SPF) wood produced by Art Massif in accordance with CSA O122-16 [14] and CSA O177-06 [15] for produce and manufacturing requirements respectively. The bracing and column elements had a stress class of 12c-E and the beam element had a stress class of 20f-Ex. The average moisture in the laboratory and of the specimen were respectively 6.6% and 6.2% during the test. The modulus of elasticity considered for 12c-E and 20f-Ex grades were 9700 MPa and 10300 MPa respectively. All the requirements from CSA O86-14 [9] were respected during the design phase of these elements.

3.2 EXPERIMENTAL SPECIMEN

The experimental frame, as shown in Figure 2, represents the braced frame at ground level of the bay perpendicular to the longest length of the standard building. The specimen is 7680 mm long centre to centre of the columns and 4540 mm high from the bottom of the column feet to the centre of the beam. Figure 3 shows the layouts of the specimen as well as the configurations of the connections. The section dimension of the bracing element and columns are 365 mm by 381.7 mm. To ease the manufacturing process and simplify the experimental setup, the beam element was oversized compared to the original plan and were made 365 mm by 555.2 mm. The common design coefficients for all the components of the specimen in respect to the CSA O86-14 standard were load-duration factor (K_D) of 1.15, service-condition factor (K_S) of 1.00, treatment factor (K_T) of 1.00 and system factor (K_H) of 1.00. The resistance of the specimen is governed by the yielding resistance of the brace connections that were assigned to be the ductile elements in the capacity design method used. The resistance of the brace assemblies was calculated to be 552 kN (factored) and 689 kN (nominal). All the other elements were designed to withstand more than the maximum force of the actuators to ensure proper load distribution in the fuses of the whole system.

Figure 2: *Full-scale wood frame*

3.3 SPECIMEN ASSEMBLY CHALLENGES

Assembly of the specimen took place in the structural laboratory of the University of Sherbrooke with the help of the lab technicians, the support of a candidate to the engineering profession and professional engineers.

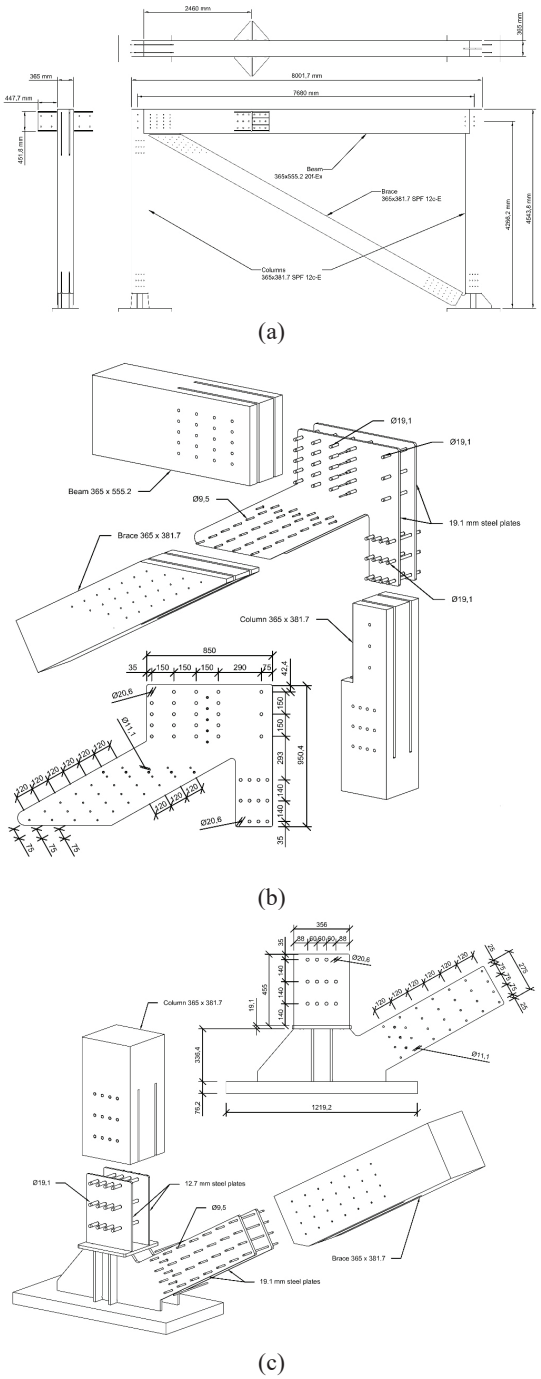

Figure 3: *Specimen layout: full-scale wood frame (a), top brace connection (b) and bottom brace connection (c)*

Some challenges occurred during the assembly due to the scale of the specimen. The wood elements arrived with an unknown degree of humidity which was approximated to be high due to the possible exterior storage of the wood slats prior to assembly. Since the laboratory is well aerated and kept dry, multiple cracks started to appear on the specimen until the day of the test. These cracks, as shown in Figure 4 (a), were carefully monitored to ensure

the integrity of all the components. After testing, the specimen was cut at precise locations to establish the depth of the cracks and none of them were identified as critical. It showed that all the cracks were on the surface only and did not change the integrity of the wood.

Another challenge was the alignment of the holes in the steel plates. Even though all the holes in the wood and in the steel were drilled by a computerized numerical control machine, some holes were not precisely aligned, as shown in Figure 4 (b). In general, the misaligned holes were forced, and the dowels passed through. However, one of the holes in the single column connection was grinded to allow the 19.1 mm dowel to pass through. It was evaluated that only one enlargement of a hole in the single column connection would not affect the results du to the scale of the specimen. It was also established that this would somehow represent errors observed on a construction site and the enlargement technique used was as per typical on-site instructions.

The beam to column connection opposite to the top corner of the diagonal element was composed of a 270 mm by 270 mm by 12.7 mm thick steel plate. A total of six dowels (three in the beam and three in the column) ensured that the pieces would stay together. This assembly was not designed to withstand forces arising from the lifting of the specimen. Therefore, a steel bracing system, as shown in Figure 4 (c), was screwed onto the specimen. Once the specimen was in its testing position and no uplift forces were applied on the beam, the steel brace was removed, and the twelve lag screw holes (six on each side) were filled with the same glue used to manufacture the wood elements. Wooden dowels were used to block the glue filled holes. No cracking was observed du to the installation of the temporary steel bracing prior to the gluing and blocking of the holes.

Since the laboratory setup did not allow for the beam to be dismounted from the simple column throughout the test, a safety block was installed. This 347 mm by 350 mm by 130 mm thick glulam block was installed on the face of the column directly under the beam as shown in Figure 4 (d). Four 8 mm in diameter by 240 mm long screws were installed at a 90-degree angle and 8 mm in diameter by 350 mm long screws were installed at a 45-degree angle. These screws ensured that the beam would be supported in the case of a detachment from the column during the pulling cycles. A clearance of approximately 2 mm was ensured between the beam and the block to allow for movements without interfering the results.

(a)

(b)

(c)

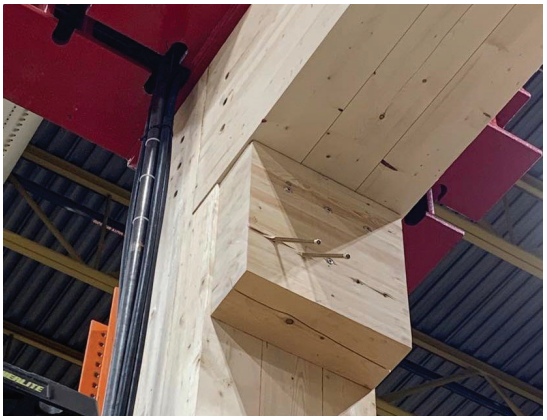

(d)

Figure 4: *Assembly challenges of the specimen: superficial cracks (a), dowel hole misalignment (b), lifting brace (c) and security block (d)*

4 EXPERIMENT PARAMETERS

4.1 TEST SET UP AND INSTRUMENTATION

The experimental setup was composed of three essential systems for the proper functioning of the laboratory tests. The guidance system ensured that the loads are appropriately transmitted to the specimen system. It also ensured that the specimen did not deviate from its lateral trajectory. All of this was documented by the

https://doi.org/10.52202/069179-0269

instrumentation system linking the specimen movements to the data collection tools.

As shown in Figure 5, the specimen was assembled horizontally and temporarily braced with additional timber elements. These braces allowed the specimen to be lifted vertically in its testing position while ensuring minimum efforts in the dowel assemblies. Columns steel bases were made of 15.9 mm and 19.1 mm thick steel plates welded to 1219.2 mm long by 609.6 mm wide and 76.2 mm thick foundation plates. These plates were anchored with high resistance steel rods to the concrete reaction floor.

(a)

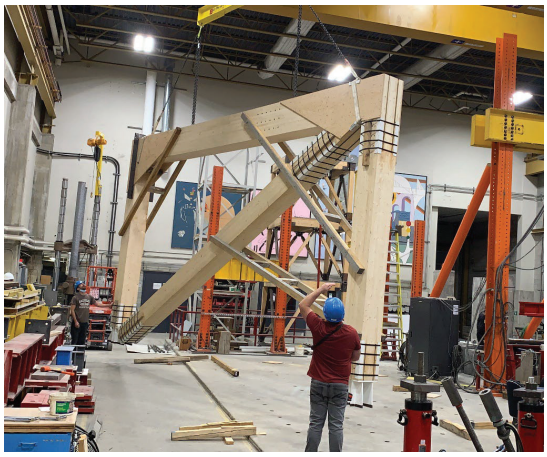

(b)

Figure 5: *Specimen bracing: bracing system (a) and lifting (b)*

A 12 m reinforced concrete reaction wall with a shear strength of 8000 kN, an overturning resistance of 25000 kNm and a punching resistance of 1500 kN was used to anchor two hydraulic actuators. The actuators were from MTS System Corporation and were controlled by the MTS FlexTest-60 system. The maximum capacity of each actuator was 500 kN and they had a displacement range of ±250 mm. The heads of the actuators were anchored to metal braces bolted into the wood beam with 18 one inch in diameter bolts. Hinges at the base and at the head of the actuators allowed to eliminate the bending moment generated by the gravity forces. To simulate the gravity load from above stories, two high-strength rods were anchored in each foundation plates to apply 292 kN of force in the long axis of each of the columns. The rods were connected to a transfer beam at the top of the columns which ensured the correct distribution of the load. The steel beams were connected to a load cell system which ensured that the loading remained constant during the test. The load variation was negligible due to the small angles generated. As shown in Figure 6, the out-of-plane bracing system was made up of four W section steel columns on which two beams were mounted. These beams included a network of rollers and guides ensuring that the specimen did not deviate from its lateral axis when subjected to a cyclic loading.

Potentiometers, linear variable differential transformers (LVDT) and load cells, as shown in Figure 7, were used to capture all the required data for the analysis of the frame's behaviour.

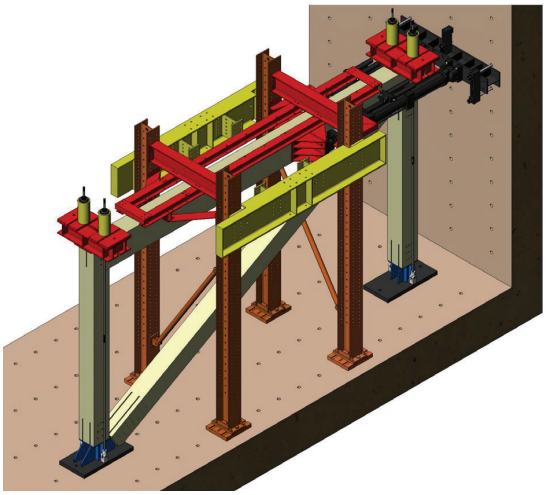

Figure 6: *Guidance system of the laboratory set up*

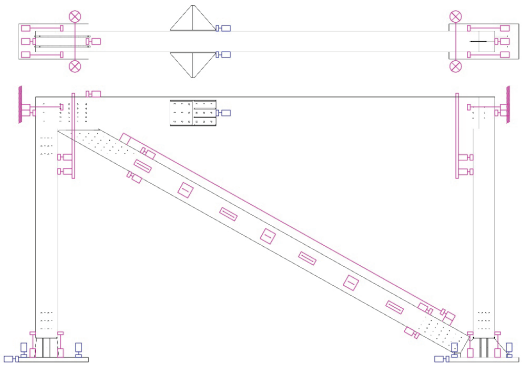

Figure 7: *Instrumentation set up*

4.2 LOADING PROTOCOL

Due to the availability of only one specimen, multiple Due to the availability of only one specimen, multiple parameters were established to ensure proper testing of

the frame. Test method A also known as the Sequential-Phased Displacement Procedure (SPD) in the protocol from the American Society of Testing and Materials E2126-19 [16] was used as a reference. The SPD method shown in Figure 8 involves multiple phases of controlled loading cycles that incrementally increase the displacement of the structure. Two patterns of reversed cyclic loading were applied to the specimens. The first displacement pattern was divided in three phases with the amplitude based on the anticipated first major event (FME). The FME was established to be the first significant limit state to occur. Each phase had a displacement of 25% (step 1), 50% (step 2) and 75% (step 3) of the anticipated FME. The second displacement pattern was composed of an initial phase, a decay phase and a stabilization phase that increased after each cyclic phase of pattern 2 is completed. The initial phase had one cycle at 100% displacement (step 4) of the anticipated FME. The decay phase had three reversed cycles that decreased the initial phase amplitude by steps of 25% of the displacement. The stabilization phase had three cycles that replicated the amplitude of the initial phase. This pattern was repeated until one of the stop criteria was achieved.

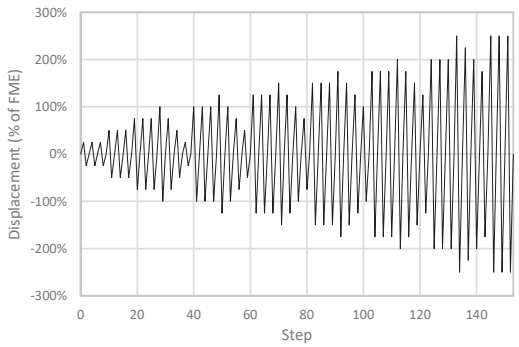

Figure 8: *Loading procedure*

Since only one specimen was available to test, no monotonic test was performed to establish the FME nor the ultimate displacement of the specimen. However, theoretical calculations based on the SIA265 standard [10], Eurocode 5 (E5) [11], E5 platform [17] and Popovski's method [12] were made to evaluate the FME. Due to the capacity design of the frame, the first major event was defined as the yield point of the dowels inside the assemblies of the frame. The lateral force of 482 kN corresponding to an assumption of a 9.21 mm drift was established as the FME for the final test. Through previous testing on large-scale wood structural members at the University of Sherbrooke, it was determined that a loading rate of 0.5 mm/s would be used. This rate was chosen based on the recommendations of the laboratory professionals, as faster loading rate would not have allowed the test to be paused before a possible critical event with potential negative impacts on the specimen. The sampling rate of the instrumentation was set at 50 readings per second.

Two preliminary cyclic load tests followed by a final destructive test were conducted. The first preliminary test (Test 5%) consisted of a triangular wave loading pattern at very low loading rate with a lateral force of 24.1 kN equivalent to 5% of the FME. The goal of the first preliminary test was to ensure proper operation of the instrumentation and loading system. The second loading test (Test 100%) consisted of steps 1 to 4 of method A controlled by force parameters. The goal of the second test was to validate the overall stiffness of the system and to confirm if the theoretical values of the FME were well evaluated. The established limits allowed to stay in the elastic domain and potentially enter the initial phase of the plastic domain. In this case, the force control of the actuators was programmed to perform a lateral thrust of 481.4 kN. Based on the results of the second test, the lateral stiffness of the system and the FME was confirmed. Then the complete loading protocol (Test final) was performed in displacement control until one of two stop criteria was achieved.

The two stop criteria were an observation of a degradation of more than 20% of the specimen's resistance and when the maximum force of 1000 kN of the actuators is achieved. The final test was terminated because the maximum force of the actuators was achieved. However, a maximum lateral force of approximately 1100 kN was applied on the specimen due to a slight increase of the laboratory hydraulic pump capacity.

5 EXPERIMENTAL OBSERVATIONS

5.1 HYSTERETIC BEHAVIOUR OF THE WHOLE FRAME

The hysteretic curves shown in Figure 9 represent the average lateral displacement of the top section of the specimen. It was calculated as the average drift of the two upper assemblies at the vertical centre line of the beam. A correction of the curve in reference to the elongation and compression of the wood was applied to ensure proper representation of the true displacement.

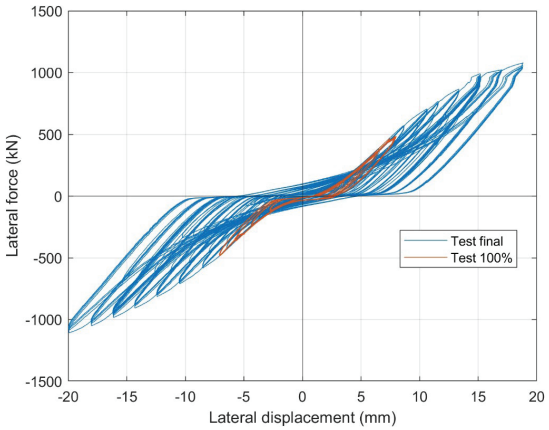

Figure 9: *Hysteresis curve*

It is observed that the curve of the Test 100% shows a very similar elastic behaviour to that of the Test final. In both tests, during return to point zero, the curves don't show any flattening, which means that the specimen remained in the linear deformation domain for both tests. An

https://doi.org/10.52202/069179-0269

average of the difference in displacements at each cycle of about 0.5 mm was recorded. This difference is explained by the fact that the 100% test was performed in force control while the final test was performed in displacement control.

Observation of the hysteresis curve past the yielding point of the brace assemblies shows a broadening of the curves that characterizes an overall ductile behaviour. The stability of each subsequent cycle demonstrates that there is a dissipation of energy increasing at a stable rate. There is also a shift in the curve before the engagement of the elements that resist the lateral force. This phenomenon is common in wood structures and can be explained du to the 1 mm clearance in the connections slots and holes to facilitate assembly. This clearance creates a slight shift in the curves when there is a change in the direction of the force.

5.2 LATERAL STIFFNESS

Lateral stiffness of the system subjected to a cyclic force is determined using the secant stiffness defined by the ratio of force to displacement as shown by the Equation 1 [18]:

$$k_i = \frac{|F_i^+| + |F_i^-|}{|X_i^+| + |X_i^-|} \quad (1)$$

where F_i^+ ; F_i^- are the peak loads of each cycle and X_i^+ ; X_i^- are the relative displacements of the same cycles.

Analysis of the stiffness curve, shown in Figure 10, shows that there is a loss in the overall stiffness of the specimen once the sequence of cycles at the FME amplitude is passed. The FME is achieved when there is a lateral displacement of 9.21 mm. In the test, an average force of approximately 576 kN was required to achieve this displacement. This corresponds to a specimen secant stiffness of 68447 kN/m.

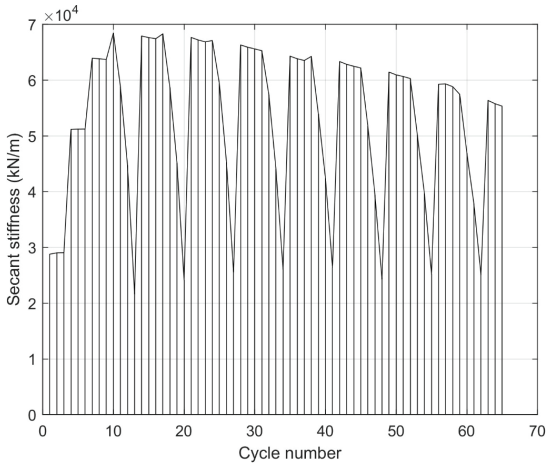

Figure 10: *Secant stiffness curve*

The curve of the following cycles shows that there is a loss of stiffness until the end of the test. Therefore, it can be established that the FME was exceeded, and that the specimen shows a behaviour with plastic failure modes. However, it should be noted that the exceedance of the elastic limit was probably achieved between the FME cycle and the next higher cycle. Hence, the CEN method [19], was used to define the slope of the envelope in the linear domain. Note that the slope (K_α) shown in Figure 11 was evaluated for comparative purposes, as it was not possible to measure the maximum strength of the specimen. As a result, the stiffness in the linear domain is estimated to be 86659 kN/m.

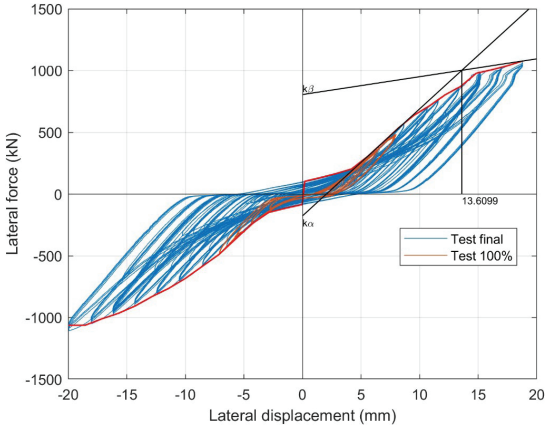

Figure 11: *Approximation of CEN method*

5.3 ENERGY DISSIPATION

The amount of energy dissipated by the specimen is determined by measuring the area of the hysteresis curve in respect of each cycle as shown by Equation 2 [20]:

$$E_{Di} = \int F_i(x)dx \quad (2)$$

where $F_i(x)$ is the hysteresis curve function in accordance with the lateral displacement.

The ratio of dissipated energy is the ability of the overall system to dissipate energy over the strain energy required to deform it. In the case where there are no mechanisms to dissipate energy, the ratio would be zero. However, at each subsequent cycle during the test, there was at least one energy dissipation mode present that ensured a ratio increase. It can be determined using Equation 3 and Equation 4 [20]:

$$E_i = \frac{E_{Di}}{2E_{S0i}} \quad (3)$$

$$E_{S0i} = \frac{k_i u_{0i}^2}{2} \quad (4)$$

where E_{S0i} is the deformation energy per cycle, k_i is the lateral stiffness of the system and u_{0i} is the maximum displacement.

The gradual increase of the energy dissipation ratio shown in Figure 12 is explained as a result of increased friction, cracking, and especially due to the yielding of the brace assemblies.

https://doi.org/10.52202/069179-0269

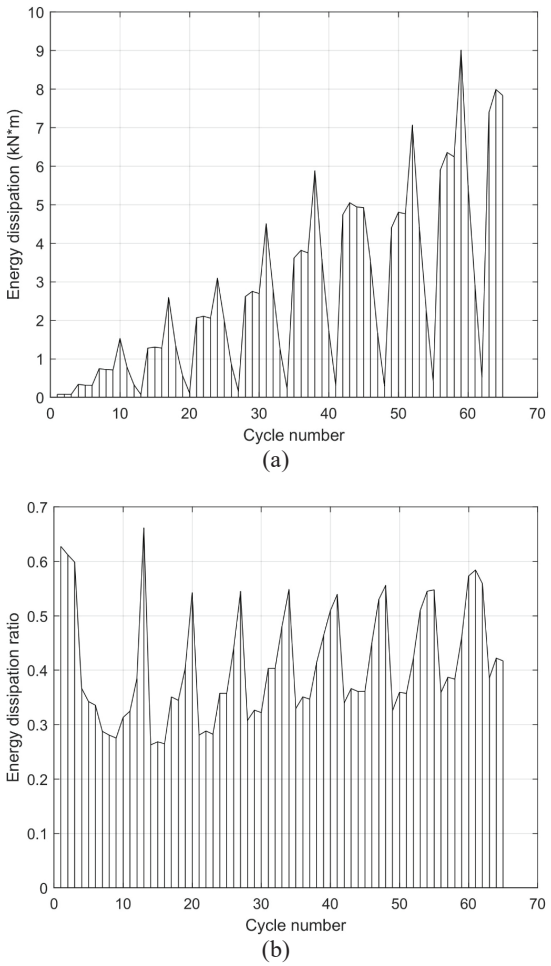

Figure 12: *Energy dissipation: energy dissipation per cycle (a) and energy dissipation ratio (b)*

5.4 STRENGTH DEGRADATION

When a structure is subjected to cyclic forces simulating the forces of earthquake aftershocks, the structure in question may suffer more damage than anticipated. That is why it becomes very important to consider the rate at which SFRS degrade in strength [21]. The degradation under cyclic loads was characterized using the degradation coefficient defined by the equation [18].

$$\lambda_i = \frac{F_i}{F_{max}} \tag{5}$$

where F_i is the force of the observed cycle in a sequence and F_{max} is the peak load of the same sequence.

As expected, the results obtained shows that all the cycles in the elastic domain of the specimen shows negligible strength degradation. Past the elastic limit, the first cycles of each phase corresponds to the maximum load of reference. The subsequent cycle shows a loss of strength due to the crushing of the wood in the connections. Figure 13 illustrates the loss of strength during the test when the lateral load is directed in the east and west directions. The strength degradation trend is relatively stable. Due to the large over-capacity, a degradation of 3.73% was observed when the maximum lateral force was applied.

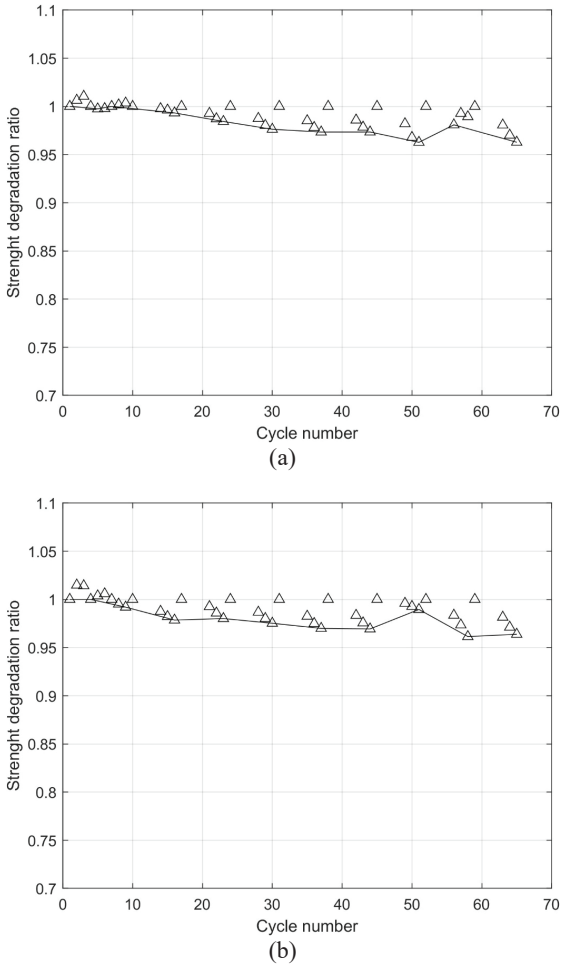

Figure 13: *Strength degradation ratio: load traveling in the east direction (a) and the west direction (b)*

5.5 R_D AND R_O MODIFICATION FACTORS

The R_d factor considers the ductility of the system and its ability to absorb energy, and the R_o factor considers of the excess in resistance of the structure. The force modulation factor R_d ensures that the structural system has the capacity to absorb energy, while having acceptable deformations. When a building is designed with a R_o factor greater than 1, it is considered that the structure can undergo inelastic deformations and that the connections can deform ductile.

According to a study [22], the modification factor R_d is defined by the equation 6.

$$R_d = \sqrt{2\mu - 1} \tag{6}$$

where μ is the ductility expressed as the ratio of displacement at failure to displacement at yield.

The ratio P_{max}/P_y is used to calculate the R_{yield} factor in the evaluation of the coefficient which considers the

https://doi.org/10.52202/069179-0269

excess strength of the structure. Equation 7 is explained in a study [23] to calculate the R_o factor.

$$R_o = R_{size} \cdot R_{\phi} \cdot R_{yield} \cdot R_{sh} \cdot R_{mech} \quad (7)$$

where R_{size} is the overstrength arising from restricted choices for sizes of elements and rounding of sizes and dimensions equal to 1.05; R_{ϕ} is the factor accounting for the difference between nominal and factored resistances equal to 1.43; R_{yield} is the ratio of actual yield strength to minimum specified yield strength; R_{sh} is the overstrength due to the development of strain hardening equal to 1.00 and R_{mech} is the overstrength arising from mobilizing the full capacity of the structure such that a collapse mechanism is formed equal to 1.00.

Since failure of the specimen was not achieved, it is important to note that the value of the displacement and force found with the method used to determine the yielding point can be improved. In addition, it is crucial to obtain the displacement and force at the point of failure in order to properly evaluate the modification factors. Thus, solely to provide an overview of the test results, the following R_d^* and R_o^* values were calculated with the results at the point of maximum force applied to the specimen. The ratio P_{max}/P_y was used to calculate the R_{yield} factor. It is important to consider that the NBCC takes a conservative approach by assuming that the R_{yield} factor is equal to 1.00. However, our tests show that the R_{yield} value is higher and therefore a larger value of the R_o^* factor would be expected. In addition, the calculated values may be considered as underestimated due to the fact that the point of failure is probably higher than the point of maximum force applied on the specimen during testing. R results from our tests lead to calculated value of R_d^* equal to 1.87 and a R_o^* value equal to 2.85.

6 CONCLUSION

Evaluating the seismic behaviour of a full-scale wood frame under cyclic loading to obtain seismic properties for optimization and better understanding of such a system was achieved during this research. The elastic performances of the specimen based on capacity design was evaluated. The following conclusions come from the observations of the specimen and the analysis of the results:

1. The overall behaviour of the system demonstrated that the use of a preliminary test in the elastic domain was an adequate method to validate the elastic stiffness of the specimen in order to establish the limits of a destructive test.
2. The braced frame system, from this research project, demonstrated the same behavior several times during the preliminary tests and during the final test in the elastic domain.
3. In comparison with the study of Xiong and Liu [5], it can be concluded that the overall behaviour of the diagonally braced structure is comparable to a K-braced bolted system.
4. An increase in the ratio of dissipated energy with increasing amplitude of each cycle is observed.
5. There is a loss of stiffness of the overall system passed the elastic limit of the fuse elements.
6. The strength degradation of the system was influenced by the yielding of the fuse elements.
7. The tests in this research project resulted in a value for the R_d^* coefficient that was close to the value established by the 2015 NBCC. The test value is underestimated and therefore a a somewhat higher value would be expected when testing to complete failure. This value would slightly exceed that of the 2015 NBCC.
8. The tests in this research project resulted in a value for the R_o^* coefficient that is much larger than the value established by the 2015 NBCC. This value is also underestimated, as tests were not completed to failure. Thus, there is room for improvement in the proposed CNBC value for system types similar to the one in this research project.
9. Based on the observations of the specimen in this research, a great deal of overstrength is associated with wood frame systems due to the oversizing of the unprotected elements.
10. A lack on information in Canadian standards about stiffness properties of steel connectors in wood was identified. Other national standards can be used to establish preliminary assumptions, but further research should be conducted to provide models with respect to Canadian materials.

In order to better understand the complete behaviour of the frame, it would be appropriate to create a numerical model using different finite element software and use the results for calibration purposes. In this way, a complete model of the SFRS and the structure could be compared to a typical design practice. These results would allow to establish the ductility of the frame and the force modification factors associated with it. To further extend the project, the calibration of such a model could lead to the dynamic finite element analysis of different types of structures with the same SRFS. Thus, these studies could establish a starting point for Canadian standards with respect to the introduction of new requirements related to the seismic behaviour of wood structures.

ACKNOWLEDGEMENT

The authors would like to acknowledge the funding from the National Sciences and Engineering Research Council of Canada and the Québec FRQNT fund. The authors also recognize Art Massif for their collaboration and funding, and for providing the frame for this project. This study was carried out in collaboration with the CIRCERB research Chair at Université Laval, and the CEISCE research centre, Finally, the authors are grateful for the technical support of the staff at Université de Sherbrooke structures laboratory.

REFERENCES

[1] Commission canadienne des codes du bâtiment et de prévention des incendies, « Code national du bâtiment – Canada 2015 », National Research Council of Canada, DOI: 10.4224/40002005, 2015.

[2] M. Popovski et E. Karacabeyli, « Force modification factors and capacity design procedures for braced timber frames », 2008.

[3] C. D. Frenette, « The seismic response of a timber frame with dowel type connections », 1997, doi: 10.14288/1.0050203.

[4] K. Gatto et C.-M. Uang, « Effects of Loading Protocol on the Cyclic Response of Woodframe Shearwalls », *Journal of Structural Engineering*, vol. 129, nº 10, p. 1384-1393, oct. 2003, doi: 10.1061/(ASCE)0733-9445(2003)129:10(1384).

[5] H. Xiong et Y. Liu, « Experimental Study of the Lateral Resistance of Bolted Glulam Timber Post and Beam Structural Systems », *J. Struct. Eng.*, vol. 142, nº 4, p. E4014002, avr. 2016, doi: 10.1061/(ASCE)ST.1943-541X.0001205.

[6] Canadian Wood Council, AKA Architecture + Design, et Art Massif, « Low-Rise Commercial Wood Building Initiative ». Canadian Wood Council, 11 décembre 2019.

[7] CSI, « SAP2000 Integrated Software for Structural Analysis and Design ». Computers and Structures Inc., Berkeley, California, United States.

[8] S-frame, « S-Frame Software Canada ». Altair Engineering Inc., Richmond, BC, Canada.

[9] CSA, « O86-14: Règles de calcul des charpentes en bois », *Canadian Standards Association, Mississauga, Canada*, 2014.

[10] Société suisse des ingénieurs et architectes, « SIA265:2012 Construction en bois ». Société suisse des ingénieurs et architectes, 1 janvier 2012.

[11] NF, « Eurocode 5 : Conception et calcul des structures en bois », *AFNOR*, 1995.

[12] Z. Chen et M. Popovski, « Expanding wood use towards 2025: Seismic perf of braced mass timber frames Yr2 », FPInnovations, févr. 2020. [En ligne]. Disponible à: https://library.fpinnovations.ca/fr/viewer?file=%2fmedia%2fWP%2f36376.pdf#search=Marjan&phrase=false

[13] CSA, « S16–19: Limit States Design of Steel Structures », *Canadian Standards Association, Mississauga, Canada*, 2019.

[14] CSA, « O122-16: Structural Glued-Laminated Timber », *Canadian Standards Association, Mississauga, Canada*, 2016.

[15] CSA, « O177-06 (R2015): Qualification Code for Manufacturers of Structural Glued-Laminated Timber », *Canadian Standards Association, Mississauga, Canada*, 2015.

[16] ASTM International, « E2126-19 Standard Test Methods for Cyclic (Reversed) Load Test for Shear Resistance of Vertical Elements of the Lateral Force Resisting Systems for Buildings », American Society for Testing and Materials, West Conshohocken, PA, 2019. doi: 10.1520/E2126-19.

[17] J.-F. Bocquet, L. Cabaton, D. Calvi, et E. Sauvignet, « Assemblages bois-métal à plans de cisaillement multiples ». Platforme Eurocode 5, 11 janvier 2013.

[18] China Academy of Building Research, « Specification of test methods for earthquake resistant building », Ministry of Construction architectural engineering standards technical focal China Academy of Building Research, JGJ101-96, déc. 1996.

[19] W. Muñoz, M. Mohammad, A. Salenikovich, et P. Quenneville, « Determination of yield point and ductility of timber assemblies: In search for a harmonised approach », Engineered Wood Products Association, Technique, 2008.

[20] P. Paultre, *Dynamics of Structures*. John Wiley & Sons, Ltd, 2013. doi: 10.1002/9781118599792.

[21] M. Popovski, H. G. L. Prion, et E. Karacabeyli, « Shake table tests on single-storey braced timber frames », *Can. J. Civ. Eng.*, vol. 30, nº 6, p. 1089-1100, déc. 2003, doi: 10.1139/l03-060.

[22] F. A. Boudreault, C. Blais, et C. A. Rogers, « Seismic force modification factors for light-gauge steel-frame - wood structural panel shear walls », *Can. J. Civ. Eng.*, vol. 34, nº 1, p. 56-65, janv. 2007, doi: 10.1139/l06-097.

[23] D. Mitchell, R. Tremblay, E. Karacabeyli, P. Paultre, M. Saatcioglu, et D. L. Anderson, « Seismic force modification factors for the proposed 2005 edition of the National Building Code of Canada », *Can. J. Civ. Eng.*, vol. 30, nº 2, p. 308-327, avr. 2003, doi: 10.1139/l02-111.

https://doi.org/10.52202/069179-0269